Ninth USA/Europe Air Traffic Management Research and Development Seminar (ATM2011)

# Analytical Workload Model for Estimating En Route Sector Capacity in Convective Weather

John Y. N. Cho, Jerry D. Welch, and Ngaire K. Underhill
MIT Lincoln Laboratory
Lexington, Massachusetts, U.S.A.
jync@ll.mit.edu, welch@ll.mit.edu, ngaire.underhill@ll.mit.edu

***Abstract*—We have extended an analytical workload model for estimating en route sector capacity to include the impact of convective weather. We use historical weather avoidance data to characterize weather blockage, which affects the sector workload in three ways: (1) Increase in the conflict resolution task rate via reduction in available airspace, (2) increase in the recurring task load through the rerouting of aircraft around weather, and (3) increase in the inter-sector coordination rate via reduction in the mean sector transit time. Application of the extended model to observed and forecast data shows promise for future use in network flow models.**

***Keywords-air traffic management; sector capacity; workload model; convective weather***

## I. INTRODUCTION AND BACKGROUND

In today's U.S. National Airspace System (NAS) en route air traffic is managed within and between discrete volumetric units known as sectors. One or more human controllers are assigned to each sector, and it is their responsibility to maintain safe and efficient traffic flow within their sector as well as to and from adjoining sectors. The dual goals of safety and efficiency are dependent on traffic density in opposing senses, with the former decreasing and the latter increasing with more traffic density. Thus, how much air traffic a sector can safely handle (sector capacity) at any given time is a crucial quantity in safely maximizing the transport of passengers and cargo throughout the NAS.

The current operational metric for sector capacity is the Monitor Alert Parameter (MAP) [1], which is a predetermined acceptable aircraft count that air traffic managers use as a gauge to limit traffic flow or increase controller staffing. The baseline MAP values are solely dependent on the average sector flight time, the rationale being that inter-sector controller workload is the main determining factor in sector capacity. The MAP rule also includes a fixed upper limit of 18 aircraft per sector, and allows discretionary adjustments of ±3 aircraft per sector as guided by operational experience.

Because air traffic management largely relies on manual procedures, controller workload determines the instantaneous maximum number of aircraft that can be safely handled in a sector [2-6]. To compute controller workload, two approaches have been taken—microscopic workload simulation [7-9] and aggregated-task analytical modeling [2, 10-14]. Although the former can take into account nearly every task imposed on the controller by a specific set of individual aircraft and flow conditions, its complexity makes it impractical to run in real time for monitor and forecast purposes. Analytical models, on the other hand, are amenable for use in tactical situations with rapidly evolving traffic flow and weather conditions. Detailed simulations are also difficult to validate and interpret as there are many task types. The aggregated-task analytical model provides less detail, but makes it easier to determine unknown parameters using experimental or operational data.

We have developed an objective and dynamically adaptable capacity estimation procedure that accounts for types of controller workload other than inter-sector coordination. This analytical sector capacity model appears to work well under fair-weather conditions [14], but does not incorporate the disruptive effects of convective weather. Weather can severely limit the capacity of the NAS. Thus, it is necessary for any practical application of a capacity model to include the effects of inclement weather conditions.

Previous attempts to include severe weather effects on en route airspace capacity have used a "fractional flow availability" approach. That is, some type of physically reasonable weather blockage on a flow is computed to yield a percentage of flow available. One model estimates individual route availability based on historical weather avoidance data in the form of a Weather Avoidance Field (WAF) [15-16]. Other approaches model flows with the fractional availability computed from the min-cut/max-flow ratio [5, 17] or areal and volumetric weather impact or severity indices [18-19]. Yet another method scans the sector with a series of parallel lines in various cardinal directions to estimate the directional permeability through weather [20]. However, none of these models consider the fundamental limitation of controller workload. Since weather hazardous to aviation residing within a sector most certainly increases the controller's workload, it is imperative to integrate such effects into a workload-based sector capacity model. In this paper we present the initial results of our effort to incorporate convective weather effects on en route sector workload.

This work was sponsored by the Federal Aviation Administration under Air Force Contract No. FA8721-05-C-0002. Opinions, interpretations, conclusions, and recommendations are those of the authors and are not necessarily endorsed by the U.S. Government.

## II. Sector Capacity Model

### A. Fair-weather Model

First, we will provide a brief review of our analytical workload model without weather effects. (See [11] for more details.) We aggregate the sector workload into four components as shown in (1),

$$G = G_b + G_r + G_t + G_c\,, \tag{1}$$

where $G$ is the total workload intensity, $G_b = 0.1$ is a constant background workload, $G_r$ is the recurring task term, $G_t$ is the sector transition workload, and $G_c$ is the conflict resolution workload. When $G$ reaches the sustainable human workload limit (0.8 according to simulation experiments [2]), the sector is deemed to have reached its capacity.

The individual workload terms other than the background workload are further decomposed into the product of the task service time and the occurrence rate.

$$G_r = \tau_r \frac{N}{P}\,, \tag{2}$$

where $\tau_r$ is the recurring task service time per flight, $N$ is the number of flights in the sector, and $P$ is the mean task recurrence period.

$$G_t = \tau_t \frac{N}{T}\,, \tag{3}$$

where $\tau_t$ is the inter-sector hand-off service time per flight and $T$ is the mean sector transit time. Finally,

$$G_c = \tau_c \frac{BN(N+1)}{Q}\,, \tag{4}$$

where $\tau_c$ is the conflict resolution task service time per flight, $Q$ is the sector airspace volume, and

$$B = 2M_h M_v V_{12}\,, \tag{5}$$

where $M_h$ and $M_v$ are the horizontal and vertical distances that constitute a separation violation and $V_{12}$ is the mean of the pair-wise closing speeds of the aircraft in the sector. (For a derivation of this expression, see [13]). The en route lateral separation standard is 5 NM, but in practice controllers add an extra margin for safety, making 7 NM a more realistic value for $M_h$. We use 7 NM for our model.

If all aircraft in a sector were flying at constant altitude, $M_v$ would be constant. Since altitude changes increase the vertical positional uncertainty of the aircraft, we correspondingly increase $M_v$ proportional to the fraction of flights that are ascending or descending in the sector. Specifically, we set

$$M_v = 1000 + F_{ca}(M_{vmax} - 1000)\ \text{ft}, \tag{6}$$

where $F_{ca}$ is the fraction of flights in the sector that changes altitude by more than 2000 ft and $M_{vmax}$ is the maximum vertical miss distance.

In (2) through (6) there are four unknown factors: $\tau_r/P$, $\tau_t$, $\tau_c V_{12}$, and $M_{vmax}$. The physical meanings of the compound factors are as follows: $\tau_r/P$ is the fraction of the total time devoted to recurring tasks per aircraft and $\tau_c V_{12}$ is the mean separation lost while resolving each conflict. In order to obtain a value for each factor, a regression analysis was performed to fit the model capacity results to observed peak daily counts for each of the 790 sectors in the 20 NAS ARTCCs [14]. The NAS-wide regression yielded values of $\tau_r/P = 0.013$, $\tau_t = 13$ s, $\tau_c V_{21} = 1.8$ NM, and $M_{vmax} = 1600$ ft. ARTCC-specific regression results were also generated.

### B. Weather Impact Model

There are many types of weather that obstruct safe and efficient flight. On landing and take-off, strong wind shears induced by microbursts are extremely dangerous to aircraft. Reduced visibility due to fog is an impediment to airport operations, and clear-air turbulence is a hazard that pilots and passengers alike prefer to avoid. Here we focus on the effects of convective weather on en route traffic management.

The main operational impact of convective weather on an en route sector is the need for aircraft to avoid airspace that is deemed dangerous. The probability that a pilot will deviate around a given level of weather severity has been quantified in the MIT Lincoln Laboratory Convective Weather Avoidance Model (CWAM) [21]. CWAM provides a gridded product, the WAF, which can be used to quantify weather blockage within a sector. We compute two-dimensional (2D) WAF values at 2000-ft altitude intervals from 25,000 ft to 45,000 ft, and integrate vertically inside the 80% WAF contours to provide an estimate of the volume of airspace blocked by the hazardous weather within each sector. Dividing by the total sector volume yields the fractional weather volume blockage, $F_w$.

The weather blockage affects the workload terms in several ways. One obvious impact is the reduction in available airspace, $Q$. Another effect is that rerouting flights around the weather blockage increases the recurring workload. If we posit that the number of aircraft requiring rerouting is $F_w N$ and that $\tau_w$ is the controller time consumed per aircraft rerouted, then we arrive at the modified workload intensity equation,

$$G = G_b + (\tau_r + \tau_w F_w)\frac{N}{P} + \tau_t \frac{N}{T} + \tau_c \frac{BN(N+1)}{Q(1-F_w)}\,. \tag{7}$$

Setting $G$ to 0.8 (the human workload limit) and solving the quadratic equation for $N$ yields the sector capacity. As $\tau_w$ is unknown, it must be determined either by observing controllers for long periods of time during severe weather or by fitting the model results to observed data. We chose to do the latter.

The number of aircraft needing rerouting due to weather, $F_w N$, is an approximation. This number can vary with the interactions between traffic flow pattern and weather morphology [18]. For forecasting purposes, however, given the large uncertainties in the weather field, we believe that this simple estimate is justified and can provide useful output for traffic management purposes.

## III. RESULTS

Validating a sector capacity model is not a straightforward task, because there is no "truth" data to which the model output can be compared. The best that we can do is to see how well the model is able to bound observed peak sector traffic counts. Even this, however, is not exact. The model should represent a sustainable sector capacity, allowing short bursts of peak count that exceed the model capacity limit. Furthermore, it is difficult to find appropriate validation cases, because the traffic count must be near theoretical fair-weather capacity before significant weather moves in—otherwise, one will not see the bounding effects of the weather on traffic. Low traffic counts can also be caused by low scheduled demand or up-stream flow restrictions. If bad weather is forecast in advance, then the air traffic managers may throttle back the demand on a sector in anticipation of a reduction in its traffic handling capacity.

With these complications in mind, we searched for severe weather events that intersected with high-traffic sectors. We looked within the pool of days from the summers of 2006-2008 for which we had archived Corridor Integrated Weather System (CIWS) [22] data and the summer of 2010 for which we had archived Consolidated Storm Prediction for Aviation (CoSPA) [23] data. The CIWS or CoSPA vertically integrated liquid water (VIL) and echo tops data were necessary for the generation of WAF data. CIWS provides up to a 2-hr forecast, while CoSPA generates up to an 8-hr forecast.

Sector airspace coordinate and traffic data were obtained from the Federal Aviation Administration (FAA) Sector Design and Analysis Tool (SDAT) [24]. SDAT archives provided the peak count (the maximum number of aircraft in a sector), the mean sector transit time ($T$), and the fraction of aircraft changing altitude by more than 2000 ft ($F_{ca}$) at 15-minute intervals. The SDAT data sets were generated in daily ARTCC-grouped sectors from 900 to 2400 UT.

Note that current WAF data are valid for altitudes above 25,000 ft. Hence, we applied our model only to en route high sectors.

### A. Results for Observed Weather Data

We discovered that sector ZDC32 was an especially good candidate for model evaluation because of its consistently heavy traffic. Fig. 1 shows results from 23 June 2006. The top plot shows the weather volume blockage by percentage. The second plot displays the mean sector transit time and the third plot is $F_{ca}$. The bottom plot compares the observed peak count with the fair-weather model capacity (blue) and weather-impacted capacity (red) for two different $\tau_w$ values.

Results from another day (21 August 2007) are shown in Fig. 2. In both cases the peak count reached the fair-weather model capacity early in the day when there was little or no weather blockage. Then when significant blockage did occur, the traffic count dropped as computed by the weather-impacted capacity model. For these (and other) cases, $\tau_w$ between 30 and 60 s appeared to make the model bound the data well.

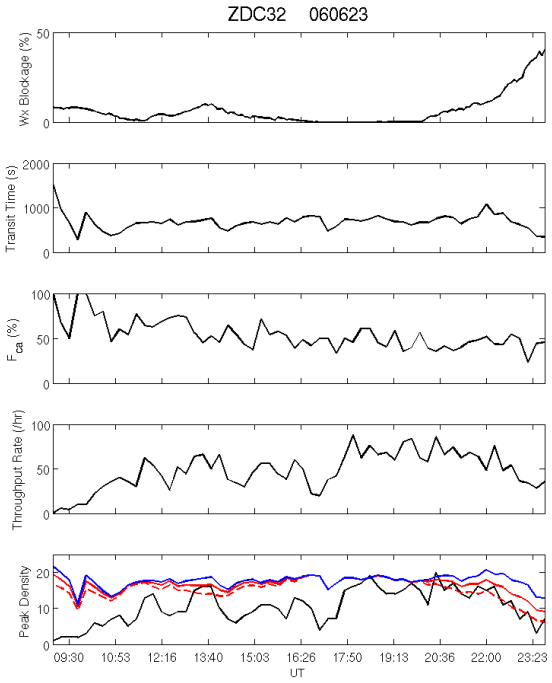


Figure 1. Data from sector ZDC32 on 23 June 2006. From top to bottom, the plots vs. time are (first) sector weather blockage volume percentage, (second) mean sector transit time, (third) fraction of sector flights that changed altitude by more than 2000 ft, (fourth) sector throughput rate per hour, and (fifth) sector peak aircraft count (black), fair-weather sector model capacity (blue), sector model capacity with $\tau_w$ = 30 s (solid red), and sector model capacity with $\tau_w$ = 90 s (dashed red).

Note also that the mean sector transit time appeared to be anticorrelated with the weather blockage. If this happens in general, it means that the weather has an effect on sector capacity not only via the two explicit terms involving $F_w$ in (7), but also indirectly through $T$ in the inter-sector coordination workload term. Operationally, a weather blockage can decrease the mean sector transit time by causing flights to exit the sector early or by forcing flights from adjacent sectors to make short intrusions into the sector under observation. The top plot of Fig. 3 shows a day on which this latter effect is observed. The bottom plot displays the weather and traffic flow situation during a time of heavy sector blockage, and flights skirting the leading edge of the storm cut across the southwest corner of ZDC32. In this way the weather blockage acted to reduce the mean sector transit time. Statistical confirmation is given in Fig. 4, which shows the relationship over all cases between normalized mean transit time ($T$ divided by the fair-weather mean sector transit time) and fractional weather blockage, $F_w$. There is a significant negative correlation between the two variables. This relationship can be used to estimate the mean sector transit time based on a forecast weather blockage.

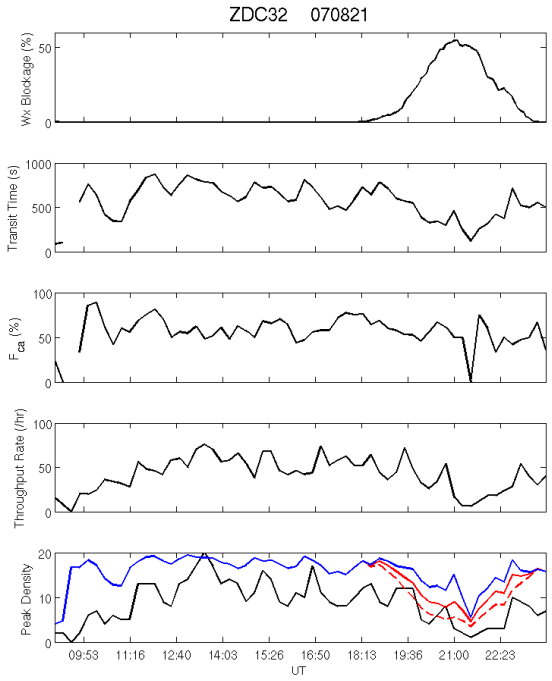


Figure 2. Same as Fig. 1 except date is 21 August 2007.

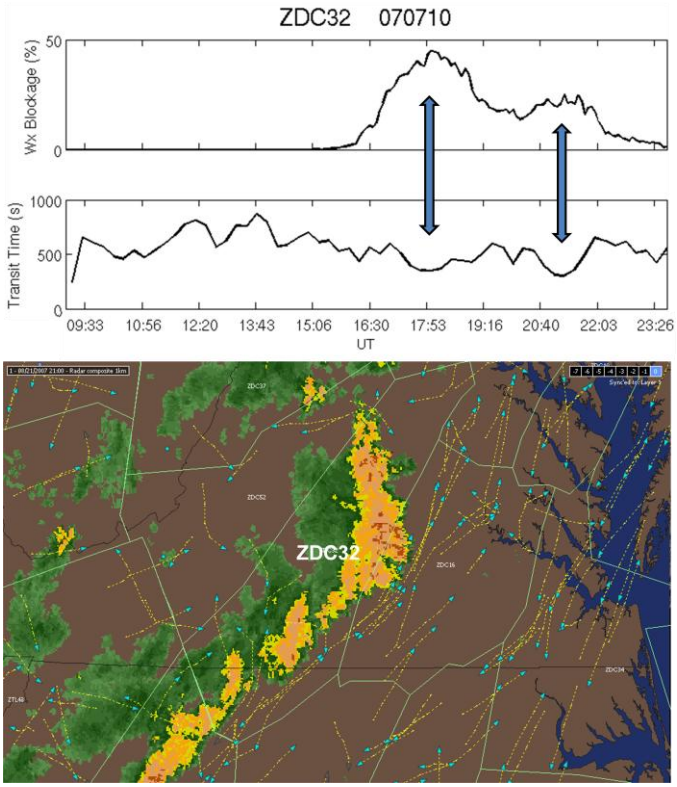


Figure 3. An example of the anticorrelation between sector weather blockage and mean transit time observed on 10 July 2007 in sector ZDC32 (top), and an overlay of flight tracks (altitude 25,000 to 35,000 ft) and NEXRAD composite reflectivity data centered around ZDC32 at 2100 UT (snapshot taken from Flight Explorer®).

A similar relationship might be expected to hold between $F_{ca}$ and $F_w$ if aircraft flying in a sector with weather blockage change their altitude to avoid the obstacle. However, this hypothesis has not been borne out by the data collected so far. Fig. 5 shows that there is no significant correlation between $F_{ca}$ and $F_w$, except perhaps a drop in $F_{ca}$ at very high weather blockages. However, the amount of data in such high blockage situations is scarce. We will revisit this issue after more cases have been identified for analysis.

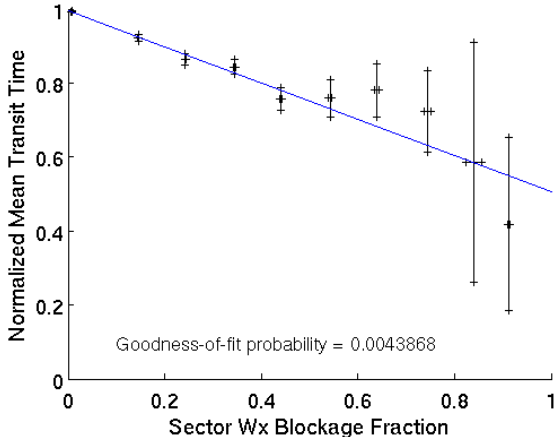


Figure 4. Normalized mean sector transit time (mean transit time divided by the average fair-weather mean transit time per sector) vs. fractional sector weather blockage ($F_w$). Data from cases listed in Table I were used. Data points were binned into 0.1 $F_w$ intervals and then averaged; the 2D error bars denote the standard deviation divided by the square root of the number of binned data. A least-squares fit using the errors in two dimensions was performed with the function "fitexy" from *Numerical Recipes* [25]. The slope of the fitted line is –0.49.

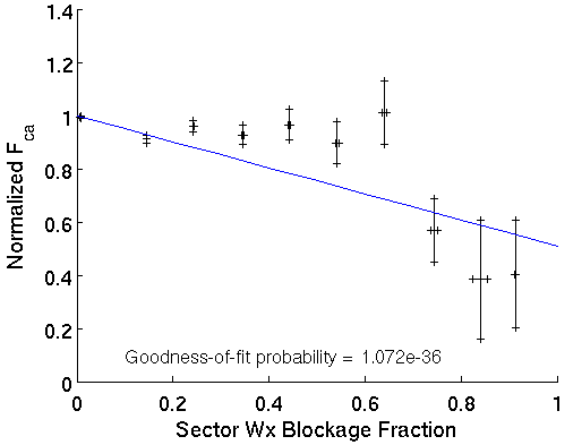


Figure 5. Normalized $F_{ca}$ ($F_{ca}$ divided by the average fair-weather $F_{ca}$ per sector) vs. fractional sector weather blockage ($F_w$). See Fig. 4 caption for methodology.

We compiled statistics from the 31 ARTCC-day cases listed in Table I. Even though we tried to concentrate on sector days with high traffic and significant weather, the SDAT data sets were grouped by ARTCCs, thus many sectors experienced no weather and/or low traffic volume. Therefore, we present the model sector capacity vs. observed peak count as 2D histograms in Fig. 6 (for $\tau_w$ = 60 s) and Fig. 7 (for $\tau_w$ = 30 s). The upper left-hand plots are essentially for fair-weather data, and as such, there is no dependence on $\tau_w$. The 1:1 line is the

model bound under which most of the data distributions fit (note that the color-map scale is logarithmic to highlight the tails of the distribution). As the weather blockage increases, the distributions shift to lower peak count/capacity values as expected, and the model continues to bound the observed data well. The number of data points also decreases with weather blockage, so for more robust statistics we need to collect more cases with heavy weather.

TABLE I. CASE LIST

| Date | ARTCC |
|---|---|
| 2006-6-1 | ZOB |
| 2006-6-2 | ZDC |
| 2006-6-14 | ZDC |
| 2006-6-21 | ZOB |
| 2006-6-23 | ZDC |
| 2006-6-26 | ZDC |
| 2006-6-27 | ZDC |
| 2006-7-5 | ZDC |
| 2006-7-12 | ZOB |
| 2006-7-22 | ZOB |
| 2006-7-26 | ZAU, ZID |
| 2006-7-27 | ZOB |
| 2007-6-27 | ZOB |
| 2007-7-10 | ZDC |
| 2007-7-17 | ZDC |
| 2007-7-19 | ZOB |
| 2007-7-20 | ZDC |
| 2007-7-25 | ZAU |
| 2007-7-26 | ZID |
| 2007-8-10 | ZBW |
| 2007-8-16 | ZOB |
| 2007-8-21 | ZDC, ZOB |
| 2007-8-26 | ZDC |
| 2007-9-27 | ZTL |
| 2008-6-4 | ZDC |
| 2008-6-12 | ZME |
| 2008-7-23 | ZDC |
| 2010-7-16 | ZHU, ZME |

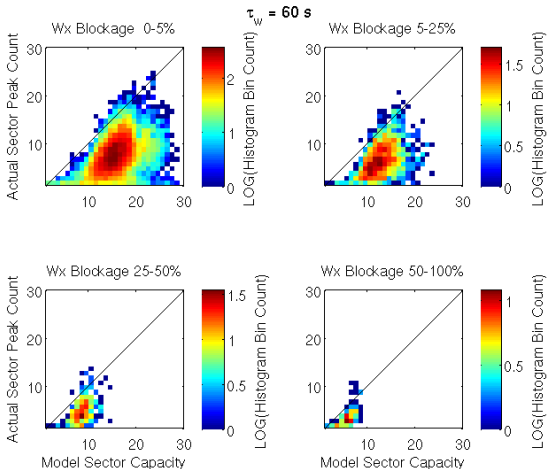


Figure 6. 2D histograms of observed sector peak count vs. model sector capacity for $\tau_w$ = 60 s. The histograms are subdivided according to different ranges of sector weather blockages as shown.

It is difficult to judge exactly what value of $\tau_w$ yields the best fit to the data. Since the model sector capacity should be a sustainable quantity, we need to allow the observed peak count to overshoot the model bound for a small fraction of the distribution. For the purposes of this paper, we have deemed $\tau_w$ = 45 s to provide a reasonable fit to the data. But in the future we will seek a more objective criterion for determining $\tau_w$. One possibility is to select a maximum acceptable "false alarm" rate, i.e., the percentage of time that the observed peak count is allowed to go over the model capacity. For example, Fig. 8 shows the percentage of observed peak counts bounded by the model. If a maximum false alarm rate of 1% is chosen, then the resulting $\tau_w$ is ~50 s. We also solicited the opinions of a former air traffic controller with many years of experience. He estimated a task completion time, assuming no communication errors, of 45-60 s to alert the aircraft, issue the reroute, verify the read-back, and complete any necessary coordination with the next sector (M. Evans, personal communication). This agrees well with our estimates.

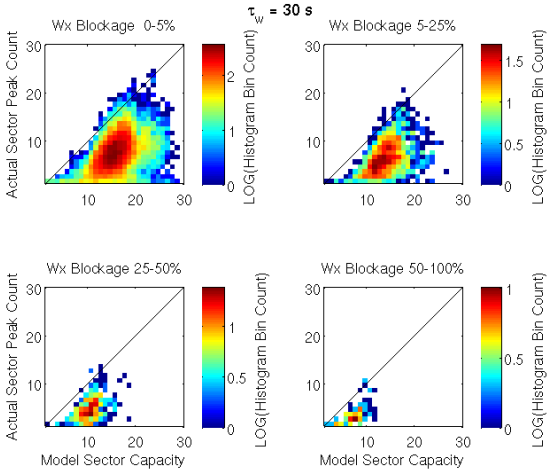


Figure 7. Same as Fig. 6 except for $\tau_w$ = 30 s.

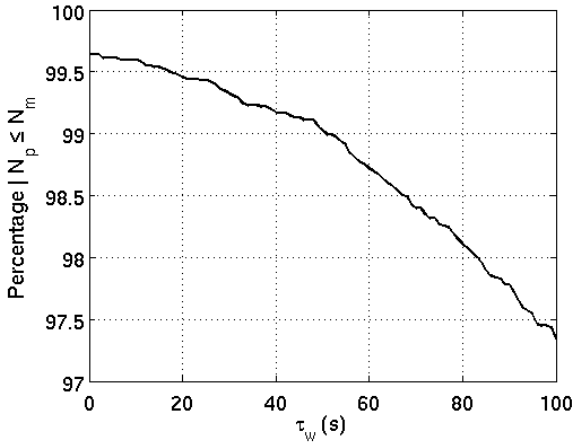


Figure 8. Percentage of observed sector peak counts bounded by the capacity model vs. $\tau_w$. Only data points with $F_w > 0$ were used.

## B. *Model Dependencies*

To illustrate the relative contribution from each of the terms in (7), Fig. 9 displays plots of workload intensity ($G$) vs. fractional weather volume blockage ($F_w$). The three rows represent sector volume increasing top to bottom, and the three columns correspond to the number of aircraft in the sector

increasing left to right. Of particular interest are the terms affected by $F_w$. The increase in conflict resolution workload due to the shrinkage in available airspace is the least significant factor, except at very high $F_w$. Under most circumstances, the weather-reroute term, with its linear dependency on $F_w$, is the most important contributor in raising the workload, followed by the increase in inter-sector coordination workload due to the decrease in mean sector transit time. This implies that when the model is used in forecast mode, it is important to have accurate predictions of baseline (fair-weather) mean sector transit times.

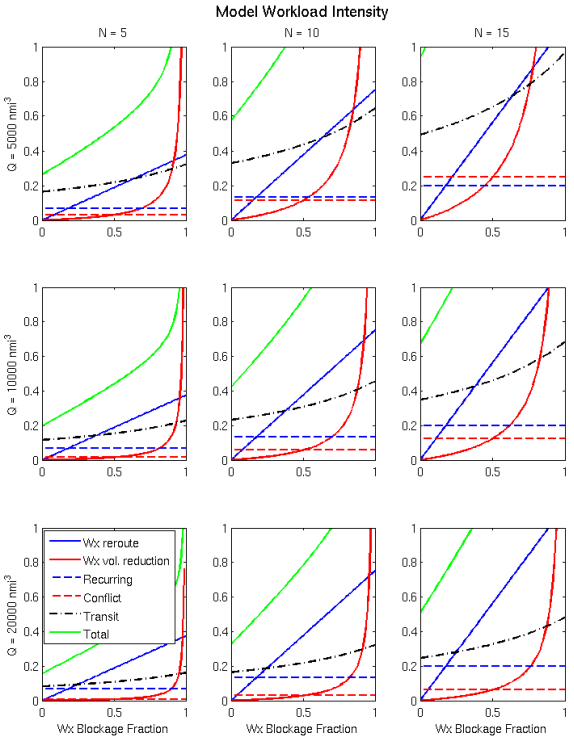


Figure 9. Plots of the individual workload terms from (7) vs. weather blockage, $F_w$. The plots are arranged according to increasing sector volume (downward) and increasing traffic count (rightward) as labeled. The conflict resolution term was decomposed into fair-weather and weather-blockage-dependent terms.

Fig. 10 summarizes the dependence of the model sector capacity on weather blockage. Without considering workload, a common estimate for the relationship between sector capacity and weather blockage fraction is a linear drop to zero capacity under total blockage conditions. However, the relationship between capacity and conflict workload is quadratic, and the actual relationship between capacity and $F_w$ is nonlinear. This figure illustrates that relationship for three different sector sizes. Here we assume that the sectors are of fixed height so that their mean transit times vary as the square root of the sector volume. NAS-averaged values are used for other model input parameters. This figure accounts for the growth in recurring service time, the linear decrease in mean transit time, and the reduction in usable sector volume with increasing weather blockage. Sector capacity declines in a roughly exponential manner until the blockage exceeds 0.8 and the resulting growth in traffic density causes conflict workload to dominate. The capacity then drops sharply to zero when the sector is totally blocked. Although the capacity dependence on $F_w$ is steeper for larger sectors, it is easier for smaller sectors to be highly blocked by weather.

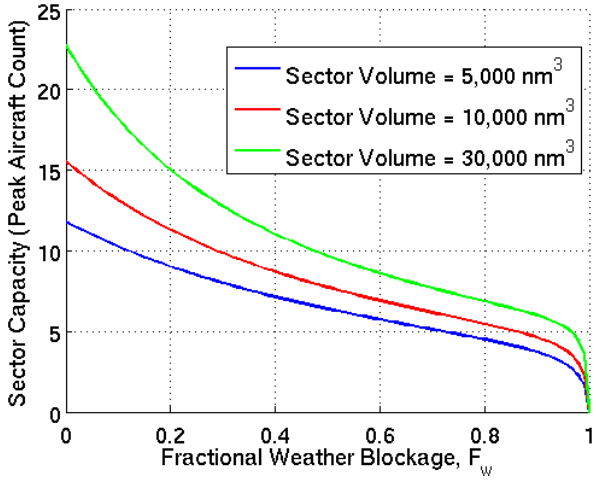


Figure 10. Model sector capacity vs. fractional weather blockage volume for varying sector volumes.

### C. *Results for Forecast Weather Data*

We now apply forecast weather data to our sector capacity model. Fig. 11 shows a case from 21 August 2007 (same as the case in Fig. 2). At that time, forecasts beyond 2 hours were not available on CIWS. In this instance, the weather blockage forecast was excellent, and the agreement between the model capacity based on observed and forecast weather is very good. For the forecast model input, long-term average values of $T$ and $F_{ca}$ for ZDC32 were used. The mean sector transit time was further modified as

$$T = T_0(1 + mF_w)\,, \tag{8}$$

where $T_0$ is the historical mean sector transit time and $m = -0.49$ is the linear slope obtained from the regression analysis of normalized mean sector transit time vs. $F_w$ demonstrated in Fig. 4. The difference between using the observed $T$ values and modified average $T$ with (8) is manifested in the variability of the blue curve vs. the smoothness of the green and red curves in the bottom plot of Fig. 11. Although the fluctuating blue curve may reflect true capacity, for operational use it would be desirable to have a smoother metric; thus, an averaged input for $T$ may be better as long as it is accurate and robust.

In the 16 July 2010 case shown in Fig. 12, however, the weather blockage forecasts were not as good. An examination of the atmospheric conditions at that time indicated a situation favorable to rapid development and decay of localized convective cells. This weather type is very difficult for current forecast models such as CoSPA to handle correctly. The tendency is to under-forecast growth and overshoot decay—hence, the distinct "time lag" seen in the forecast curves in Fig. 12. The consequence, in this case, was the increasing over-forecast of sector capacity as the forecast horizon increased.

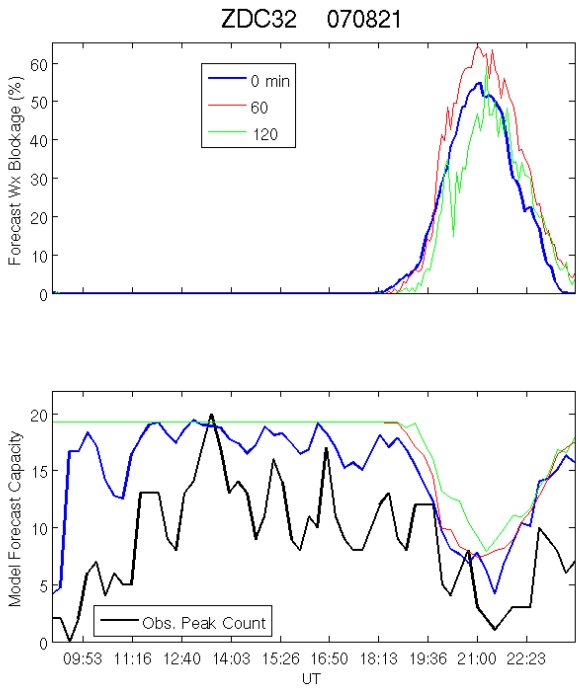


Figure 11. Plots of forecast fractional sector volume weather blockage (top) and forecast sector capacity compared with observed peak count (bottom). The line colors correspond to output using observed (blue), 1-hr forecast (red), and 2-hr forecast (green) weather.

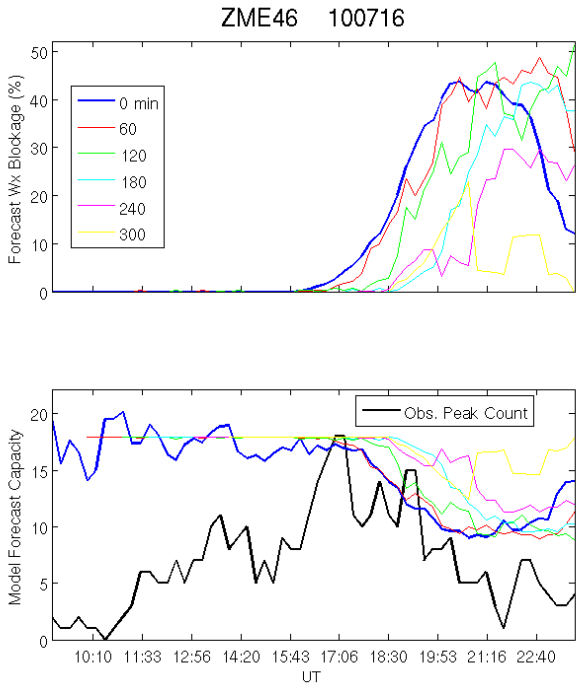


Figure 12. Plots of forecast fractional sector volume weather blockage (top) and forecast sector capacity compared with observed peak count (bottom). The line colors correspond to output using observed (blue), 1-hr forecast (red), 2-hr forecast (green), 3-hr forecast (cyan), 4-hr forecast (magenta), and 5-hr forecast (yellow) weather.

To quantify the weather blockage forecast errors, we compiled statistics for the year 2010 cases in Table I plus six other ARTCC-days (2010-6-16, 2010-7-19, and 2010-7-20 ZDC; 2010-9-16 ZNY and ZOB; and 2010-7-16 ZTL). These additional cases were not included in the earlier analyses, because the traffic was light. We included only days from year 2010, because all earlier cases were limited to 2-hr forecasts. (Note that because sector weather blockage is a scalar quantity derived from volumetric averaging, we do not encounter the usual degree of difficulty with weather forecast validation of evaluating spatial misalignments.)

Fig. 13 displays scatter plots of forecast vs. observed fractional sector weather blockage. The tight cluster around the 1:1 line starts to break up rather precipitously after 1 hour. The statistical summary given in Fig. 14 shows that the correlation coefficient falls below 0.5 after 2 hours and that a noticeable negative bias develops. Because many of the cases collected here occurred during situations of localized convective storms, we would expect the long-range forecast statistics to improve with the inclusion of more cases of widespread synoptic-scale systems that are easier to forecast.

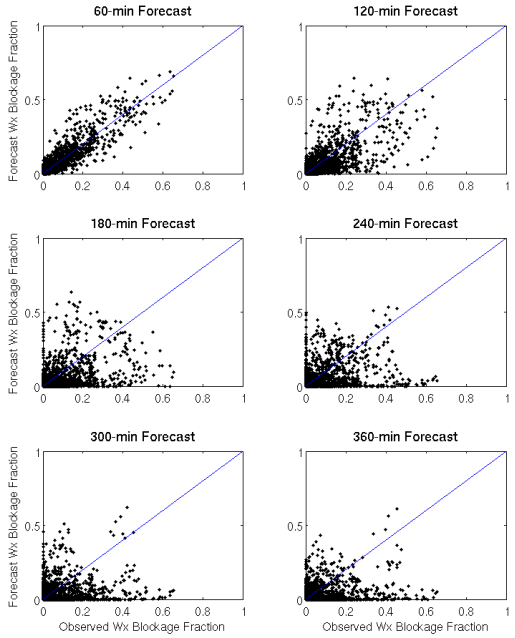


Figure 13. Scatter plots of forecast fractional sector weather blockage vs. observed fractional sector weather blockage.

It is not possible to do an analogous forecast error analysis for sector capacity, because the true sector capacity is unknown. Instead, we can only compare the sector capacity forecast to the sector capacity estimated using observed weather blockage, mean sector transit time, and $F_{ca}$. The scatter plots of these comparisons are shown in Fig. 15.

In Fig. 16 we plot the contributions of the different model input terms to the forecast error statistics. For these data, it appears that the largest error contribution comes from the uncertainties in the mean sector transit time (the difference between the blue and red curves is larger than the difference between zero error/unity correlation and the blue curves). There is a significant positive bias in the forecast that is caused by overestimates in mean sector transit times, which implies that the fair-weather-averaged values of $T$ tended to be longer

than those encountered in the study cases. The error caused by the uncertainty in $F_{ca}$ is negligible (the red and black curves are virtually equivalent). Note, however, that many of these days experienced very small fractions of weather volume blockage. This naturally biases the weighting of the total error away from the weather forecast error. If the data are filtered for strong weather blockage only, then the weather uncertainty contributions grow larger as expected. In any case, the importance of accurately forecasting the mean sector transit time is clear, for fair-weather and weather-impacted sector capacity forecasts alike.

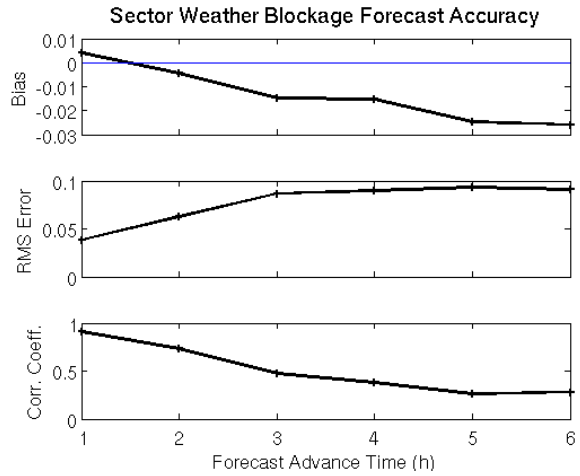


Figure 14. Plots of forecast fractional sector weather blockage bias (top), rms error (center), and correlation coefficient (bottom) relative to observed values for 1- to 6-hr forecasts.

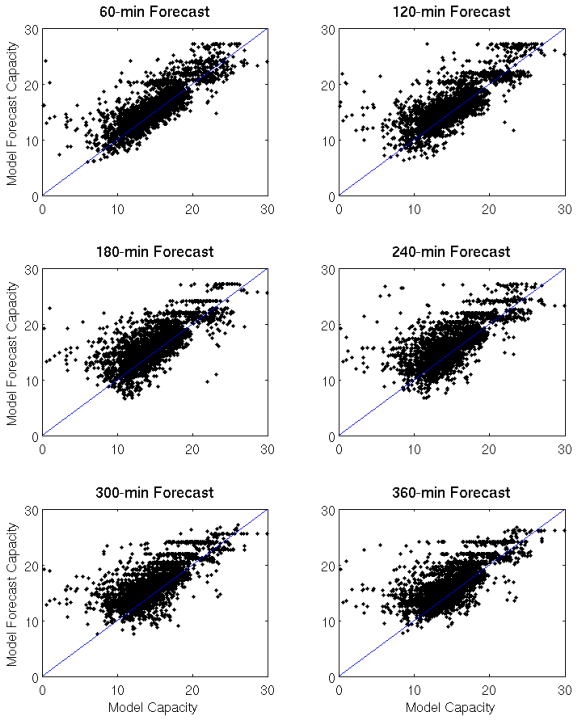


Figure 15. Scatter plots of forecast sector capacity (vertical axis) vs. sector capacity estimated using observed $F_w$, $T$, and $F_{ca}$ (horizontal axis).

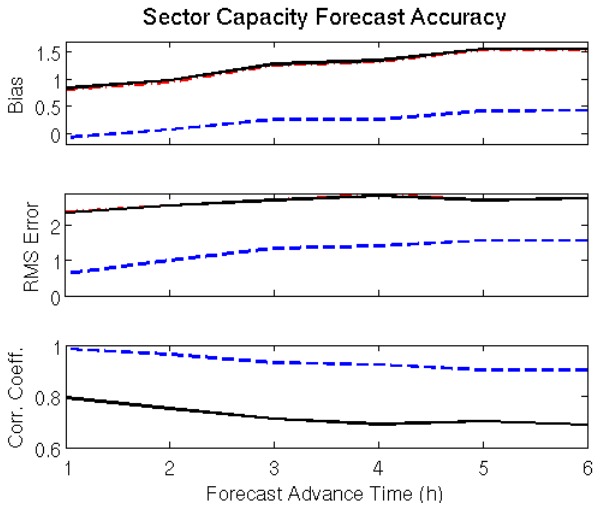


Figure 16. Plots of sector capacity forecast bias (top), rms error (center), and correlation coefficient (bottom) relative to sector capacity estimated using observed $F_w$, $T$, and $F_{ca}$ for 1- to 6-hr forecasts. The dashed blue line is for forecasts using observed $T$ and $F_{ca}$ and forecast $F_w$. The red dash-dotted line is for forecasts using observed $F_{ca}$, forecast $F_w$, and fair-weather mean $T$ (adjusted for weather blockage with (8)). The solid black line is for forecasts using historical mean $F_{ca}$, forecast $F_w$, and fair-weather mean $T$ (adjusted for weather blockage with (8)). Note that the black and red curves are nearly indistinguishable.

## IV. Discussion

Extending our sector capacity model to include convective weather impacts yielded reasonable results with observed input data. Using this model in forecast mode, however, presented additional complications. Two major factors contribute to uncertainty in the capacity forecast: (1) predicted mean sector transit time and (2) fractional weather blockage forecast. The first factor influences capacity forecasts whether or not there is weather blockage present. The leverage that $T$ has on capacity estimation can be seen in the black dash-dotted curves in Fig. 9, the differences between the blue curve and the forecast curves in Fig. 11 and Fig. 12, and the difference between the blue and the red curves in Fig. 16. (It could be argued, however, that the mean sector transit time input to the model should always be smoothed for operational use, since a fluctuating estimate of capacity would be difficult to use.) As the MAP values are explicitly based on (constant) estimates of $T$, this strong relationship has long been acknowledged. Thus, for our sector capacity model to yield significantly improved forecasts relative to the static MAP forecasts in both fair and inclement weather, accurate and reliable forecasts of mean sector transit time are needed. Since $T$ is dependent on flow patterns, this means that future demand must be modeled well.

Uncertainties in weather forecasts are dependent on weather type. The example forecast cases analyzed statistically (Fig. 13 and Fig. 14) were dominated by localized convective storms, which were not well forecast beyond 2 hours. Better accuracy beyond that time frame will typically be obtained for larger-scale synoptic disturbances. (We will check this assertion in future studies.) It is not clear how much more overall improvement can be expected in the next decade or so in weather forecast accuracy over the time and spatial scales of interest. This is one of the arguments against investing

significant effort into developing an elaborate airspace capacity forecast model, since models are only as good as the input data that go into them. Under the Next Generation Air Transportation System (NextGen), however, automation of separation assurance may reduce controller workload so that sectors much larger than those of today ("super sectors") may be formed [26]. Integrated over these larger scales, multiple-hour weather blockage volume forecast accuracy may be good enough for useful application to operational capacity forecasts.

Although it is not exactly an apples-to-apples comparison, it is encouraging that the forecast errors in Fig. 16 are less than the heuristically adjustable ±3 aircraft range of the MAP threshold.

Another issue that must be addressed (in general) is one of directional capacity. The capacity metric used in this paper (and as represented by the MAP) is a scalar value of aircraft count within a volume. Although the historical mean sector transit time for an elongated sector confers some information about flow direction, it does not explicitly specify how many flights are allowed to go in one direction or another. Consider the cartoon illustration of Fig. 17. This hypothetical sector elongated in the east-west direction to accommodate major flow in that orientation has a north-south line storm blocking its middle. The fractional volume blockage is small, so the sector capacity is not diminished significantly. However, because there is no physical gap through which aircraft can fly east-west within the sector, the flow capacity in that direction is essentially zero. This does not mean that the sector capacity model is wrong. The theoretical capacity for the north-south flow will be correct if the mean transit time is consistent with that flow direction. But in practice, because most of the demand is normally east-west, the maximum peak count is unlikely to reach the model capacity. Therefore, for operational use where directionality is important, knowledge of the sector capacity may need to be complemented by a model for directional flow limits, possibly via application of one of the existing techniques [5, 15-20]. In a network flow model each sector could perhaps be modeled by a combination of scalar "capacitance" and directional "resistances."

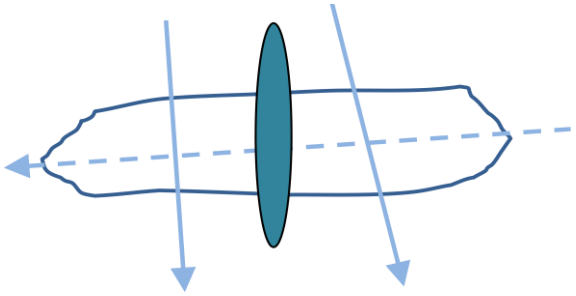

Figure 17. Illustration of a sector elongated in the east-west direction along the major flow. A line storm bisects it blocking the east-west flow, but allowing north-south flights.

Before modifying the model for directionality we will determine the frequency of occurrence of narrow, impermeable storms of the type illustrated in Figure 17. If they rarely occur, the scalar model will suffice. If they occur frequently and are predictable, knowledge of trajectory directionality may allow us to adequately forecast their effect on directional capacity.

An additional point can be made with Fig. 17 sans the weather blockage. However much one would like sector capacity to be independent of demand, such is not the case. (The same observation has been made from a flow complexity viewpoint [5].) As pointed out earlier, the capacity is strongly dependent on the mean sector transit time. If most of the traffic through the sector in Fig. 17 is flowing east-west, then the capacity is much greater than if most of the traffic flows north-south. This is the reason why sectors are elongated in the direction of the major flow. Again, this points out the need for accurate and reliable forecasts of mean sector transit time, i.e., future demand patterns.

## V. Conclusion

We have extended our analytical workload model for sector capacity estimation to include the impacts of convective weather. The airspace blockage induced by severe weather affects the controller workload equation in three ways (in order of decreasing importance): Increase in the recurring task load through the rerouting of aircraft around weather, increase in the inter-sector coordination rate via reduction in the mean sector transit time, and increase in the conflict resolution task rate via reduction in the available airspace.

The model was tested on high-altitude en-route sector data. Comparisons between observed sector peak counts and model-estimated capacity yielded reasonable results, both case-by-case and statistically. More case data, especially with high weather blockages, will be identified and analyzed in the future.

We also compared model capacity estimates using observed input vs. forecast input data. The uncertainty in forecast mode depended largely on weather blockage forecast and predicted mean sector transit time errors. The latter factor degrades fair-weather capacity estimates as well. Improving the forecast accuracy and robustness of these model input parameters will be the key to making this model useful for operational use.

## Acknowledgment

We would like to thank Mike McKinney and Joseph Post of the FAA for supporting this work.

## References

[1] Federal Aviation Administration, "Monitor alert parameter," in Air Traffic Organization Policy Order JO 7210.3W, U.S. Dept. of Transportation, Washington, DC, 2010, http://www.faa.gov/air_traffic/publications/atpubs/fac/1708.html.

[2] D. K. Schmidt, "A queueing analysis of the air traffic controller's work load," IEEE Trans. Systems, Man, Cybernetics, vol. SMC-8, pp. 492-498, June 1978.

[3] G. B. Chatterji and G. Sridhar, "Measures for air traffic controller workload prediction," 1st AIAA Aircraft Technology Integration and Operations Forum, Los Angeles, CA, 2001.

[4] P. Kopardekar, A. Schwartz, S. Magyarits, and J. Rhodes, "Airspace complexity measurement: An air traffic control simulation analysis," 7th USA/Europe Air Traffic Management Research and Development Seminar, Barcelona, Spain, July 2007.

[5] L. Song, C. Wanke, and D. Greenbaum, "Predicting sector capacity for TFM," 7th USA/Europe Air Traffic Management Research and Development Seminar, Barcelona, Spain, July 2007.

[6] S. Zelinski and T. Romer, "Estimating capacity requirements for air transportation system design," 7th USA/Europe Air Traffic Management Research and Development Seminar, Barcelona, Spain, July 2007.

[7] D. G. Denery, H. Erzberger, T. J. Davis, S. N. Green, and B. D. McNally, "Challenges of air traffic management research: Analysis, simulation, and field test," AIAA-1997-3832, AIAA Guidance, Navigation, and Control Conf., New Orleans, LA, 1997.

[8] V. Sud, C. Wanke, C. Ball, and L. Carlson-Rhodes, "Air traffic flow management—Collaborative routing coordination tools," AIAA-2001-4112, AIAA Guidance, Navigation, and Control Conf., Montreal, Canada, 2001.

[9] A. Majumdar, W. Ochieng, and J. Polak, "Estimation of European airspace capacity from a model of controller workload," J. Navigation, vol. 55, pp. 381-403, 2002.

[10] D. K. Schmidt, "On modeling ATC work load and sector capacity," J. Aircraft, vol. 13, July 1976.

[11] J. D. Welch, J. W. Andrews, B. D. Martin, and B. Sridhar, "Macroscopic workload model for estimating en route sector capacity," 7th USA/Europe Air Traffic Management Research and Development Seminar, Barcelona, Spain, 2007.

[12] J. D. Welch, J. W. Andrews, B. D. Martin, and E. M. Shank, "Applications of a macroscopic model for en route sector capacity," AIAA Guidance, Navigation, and Control Conf., Honolulu, HI, August 2008.

[13] J. D. Welch and J. W. Andrews, "Macroscopic capacity model with individual sector closing speed estimates," 9th AIAA Aviation, Technology, Integration, and Operations Conf., Hilton Head, SC, September 2009.

[14] J. Welch, J. Andrews, and J. Post, "Validation of en route capacity model with peak counts from the US National Airspace System," EN-012, 2nd ENRI International Workshop on ATM/CNS, Tokyo, Japan, 2010.

[15] B. Martin, "Model estimates of traffic reduction in storm impacted en route airspace," 7th AIAA Aviation, Technology, Integration, and Operations Conf., Belfast, Ireland, 2007.

[16] M. Robinson, R. A. DeLaura, B. D. Martin, J. E. Evans, and M. E. Weber, "Initial studies of an objective model to forecast achievable Airspace Flow Program throughput from current and forecast weather information," Project Rep. ATC-343, MIT Lincoln Laboratory, Lexington, MA, 52 pp., 2008.

[17] J. Krozel, J. S. B. Mitchell, V. Polishchuk, and J. Prete, "Maximum flow rates for capacity estimation in level flight with convective weather constraints," Air Traffic Control Quarterly, vol. 15, no. 3, pp. 209-238, 2007.

[18] L. Song, D. Greenbaum, and C. Wanke, "The impact of severe weather on sector capacity," 8th USA/Europe Air Traffic Management Research and Development Seminar, Napa, CA, 2009.

[19] J. Krozel, J. S. B. Mitchell, V. Polishchuk, and J. Prete, "Capacity estimation for airspace with convective weather constraints," 9th AIAA Aviation, Technology, Integration, and Operations Conf., Hilton Head, SC, September 2009.

[20] A. Klein and L. Cook, "Airspace availability estimation for traffic flow management using the scanning method," 27th IEEE/AIAA Digital Avionics Systems Conf., St. Paul, MN, 2008.

[21] R. A. DeLaura, M. Robinson, M. L. Pawlak, and J. E. Evans, "Modeling convective weather avoidance in enroute airspace," 13th AMS Conf. on Aviation, Range, and Aerospace Meteorology, New Orleans, LA, 2008.

[22] J. E. Evans and E. R. Ducot, "Corridor Integrated Weather System," Linc. Lab. J., vol. 16, pp. 59-80, 2006.

[23] M. M. Wolfson, W. J. Dupree, R. M. Rasmussen, M. Steiner, S. G. Benjamin, and S. S. Weygandt, "Consolidated Storm Prediction for Aviation (CoSPA)," Proc. 2008 Integrated Communications, Navigation, and Surveillance Conf., pp. 1-19, 2008.

[24] K. Geisinger and B. MacLennan, "Sector Design Analysis Tool (SDAT) workload model design document," Operations Research Service, AOR-200, Federal Aviation Administration, 1994.

[25] W. H. Press, S. A. Teukolsky, W. T. Vetterling, and B. P. Flannery, Numerical Recipes in C, 2nd ed. New York, NY: Cambridge Univ. Press, 1992.

[26] H. Erzberger and R. A. Paielli, "Concept for next generation air traffic control system," Air Traffic Control Quarterly, vol. 10, no. 4, pp. 355-378, 2002.

## AUTHOR BIOGRAPHIES

**John Y. N. Cho** holds a B.S. (1985) and M.S. (1986) from Stanford University and a Ph.D. (1993) from Cornell University in electrical engineering.

He is a Technical Staff member in the Weather Sensing Group at MIT Lincoln Laboratory (2002-present). He was a Research Scientist in the Earth, Atmospheric, and Planetary Sciences Department at MIT (1997-2002), a Research Associate at the Arecibo Observatory (1993-1997), and a Visiting Scientist at the Leibniz Institute for Atmospheric Physics (summer 1996). He has over forty publications in refereed journals.

Dr. Cho is a member of the American Meteorological Society and the American Geophysical Union.

**Jerry D. Welch** holds a B.S. and M.S. (1960) from MIT and a Ph.D. (1973) from Northeastern University in electrical engineering.

He is a Senior Staff member in the Surveillance Systems Group at MIT Lincoln Laboratory in Lexington, Massachusetts (1962-present). He helped establish the team that developed the Mode S beacon system for the FAA. He initiated the Traffic Alert and Collision Avoidance System surveillance program. He organized an Air Traffic Automation Group that helped establish programs in Terminal ATC Automation and Runway Status Lights.

Dr. Welch is a member of the American Institute of Aeronautics and Astronautics.

**Ngaire K. Underhill** holds a B.S. (2008) from Smith College in computer science and economics.

She is an Assistant Staff member in the Weather Sensing Group at MIT Lincoln Laboratory (2008-present). Her other work includes analyses on weather conditions for departure routes for aircraft particularly involving the Route Availability Planning Tool, air traffic flow patterns, and aircraft rerouting operations.